Chapter Four

Temperature-Pressure Profiles

4.1 A MYRIAD OF ATMOSPHERIC EFFECTS: GREENHOUSE WARMING AND ANTI-GREENHOUSE COOLING

Fundamentally, we would like to have full knowledge of the thermal structure of an atmosphere, as it has a major influence on computing its observed properties. Specifically, we would like to measure or infer how the temperature varies with altitude or pressure and how this *temperature-pressure profile* is altered by effects associated with the atmospheric opacities, aerosols or clouds, etc. We would like to know how a low or high albedo influences it. For Earth and the Solar System bodies, the temperature-pressure profile may actually be measured via satellite or in-situ probes. For exoplanets, this task is a lot harder and we need to resort to indirect methods.

In the absence of data on an exoplanetary atmosphere, astronomers typically label an exoplanet using its *equilibrium temperature*

$$T_{\rm eq} \equiv T_\star \left(\frac{R_\star}{2a}\right)^{1/2} (1 - A_{\rm B})^{1/4}, \tag{4.1}$$

which is the temperature equivalent to the incident starlight received by it and spread out over all 4π steradians. It is a quantity that may be computed *independent* of the properties of the atmosphere. Here, $T_\star$ is the stellar effective temperature, $R_\star$ is the stellar radius, a is the exoplanet-star separation and $A_{\rm B}$ is the Bond albedo. Our Solar System provides stunning counter-examples to this simplistic approach: Earth's equilibrium temperature is below the freezing point of water and Venus's is not much higher. In reality, the Earth hosts liquid water and Venus is an inferno with temperatures reaching about 700 K.

The reason why these equilibrium temperature estimates are so far off from reality is that atmospheres generally have a myriad of opacity sources that introduce warming and cooling effects. Absorption of radiation by atmospheric gases such as water, carbon dioxide and methane tend to produce *greenhouse warming*. Enhanced absorption or the scattering of starlight tends to produce *anti-greenhouse cooling*. Scattering of thermal emission of the exoplanet introduces the *scattering greenhouse effect*, where infrared radiation is redirected, via scattering, back towards the exoplanet [61, 117]. Aerosols or clouds complicate this picture as they possess some combination of these attributes and produce both cooling and heating, depending on their intrinsic properties and geometric

configuration [191]. We would like to understand this richness of behavior without resorting to—or in advance of—a full-blown computer simulation. Like Ray Pierrehumbert [191], my belief is that true understanding starts from simple, clear models that isolate salient behavior.

A body of work exists in the astrophysical literature on temperature-pressure profiles of irradiated exoplanetary atmospheres [79, 81, 107, 208], including my own [88, 94]. In this chapter, we will use these analytical models to reproduce the effects previously mentioned and develop an intuition for them.

4.2 THE DUAL-BAND OR DOUBLE-GRAY APPROXIMATION

To render the radiative transfer equation amenable to analytical solution, we make the approximation that the starlight incident upon the exoplanet and its thermal emission occur at distinctly different wavelengths, known as the *dual-band* or *double-gray* approximation. This is not an unreasonable approximation, since Wien's law[1] tells us that the peak wavelength of blackbody emission depends on the temperature,

$$\lambda_{\text{peak}} \approx 0.5 \ \mu\text{m} \left(\frac{T}{6000 \text{ K}} \right)^{-1}. \tag{4.2}$$

The preceding estimate applies to a Sun-like star. For Earth ($T \approx 300$ K), we have $\lambda_{\text{peak}} \approx 10$ μm, while a hot exoplanet ($T \approx 1500$ K) has $\lambda_{\text{peak}} \approx 2$ μm. The dual-band approximation appears to hold quite well.

We shall term the range of wavelengths corresponding to stellar heating the *shortwave* and subscript all associated quantities with an "S." The range of wavelengths associated with the thermal emission of the exoplanetary atmosphere is termed the *longwave*; the corresponding subscript is "L." Typically, the shortwave and longwave occur in the visible and infrared, respectively. However, it is possible for both of them to be in the infrared. For example, M stars or red dwarfs have effective temperatures of about 3000 K or lower, which means their blackbody emission peaks in the near-infrared.

The zeroth, first and second moments of the intensity are

$$\begin{aligned} J_{\text{S}} &\equiv \int_{\text{S}} J \, d\lambda, \ F_{\text{S}} \equiv \int_{\text{S}} F_{-} \, d\lambda, \ K_{\text{S}} \equiv \int_{\text{S}} K_{-} \, d\lambda, \\ J_{\text{L}} &\equiv \int_{\text{L}} J \, d\lambda, \ F_{\text{L}} \equiv \int_{\text{L}} F_{-} \, d\lambda, \ K_{\text{L}} \equiv \int_{\text{L}} K_{-} \, d\lambda. \end{aligned} \tag{4.3}$$

Note the use of the total intensity versus the net flux and radiation pressure.

[1] Wien's law states that the peak wavelength of a blackbody curve and its temperature are related via a constant number: $\lambda_{\text{peak}} T = 2.8977729 \times 10^3$ μm K.

4.3 THE RADIATIVE TRANSFER EQUATION AND THE SCATTERING PARAMETER

We wish to set up the governing equations for the temperature-pressure profiles, but we do not need to start again from the radiative transfer equation. Instead, we will invoke the two-stream treatment, which takes the moments of the radiative transfer equation (Chapter 3). Specifically, we recall equations (3.46) and (3.52),

$$\begin{aligned} \frac{\partial F_-}{\partial \tau} &= (1-\omega_0)\,(J - 4\pi B)\,, \\ \frac{\partial K_-}{\partial \tau} &= F_+\,(1-\omega_0 g_0)\,, \end{aligned} \tag{4.4}$$

but written in terms of the non-slanted optical depth (τ). In other words, τ is the optical depth measured from the top of the atmosphere to some point within it along a straight path.

To study the effects of varying the atmospheric opacities, we need to define a new coordinate other than τ. If we express the single-scattering albedo in terms of the absorption ($\kappa_{\rm a}$) and scattering ($\kappa_{\rm s}$) opacities, we obtain

$$\omega_0 = \frac{\kappa_{\rm s}}{\kappa_{\rm a} + \kappa_{\rm s}}. \tag{4.5}$$

We may show that the extinction opacity ($\kappa_{\rm e} \equiv \kappa_{\rm a} + \kappa_{\rm s}$) takes the form,

$$\kappa_{\rm e} = \frac{\kappa_{\rm a}}{1-\omega_0}. \tag{4.6}$$

Thus, the optical depth may be expressed in terms of

$$d\tau = \kappa_{\rm e}\, d\tilde{m} = \frac{\kappa_{\rm a}}{1-\omega_0}\, d\tilde{m}, \tag{4.7}$$

where $\tilde{m}$ is the column mass of the atmosphere. We write it in this manner, because it allows for the absorption and scattering to be described by $\kappa_{\rm a}$ and ω_0, respectively. The absorption opacity and single-scattering albedo may now be used as input parameters, while the column mass serves as a coordinate. We have essentially separated out the opacities, which are microscopic quantities, from the pressure coordinate of the atmosphere.

It follows that the equations in (4.4) become

$$\begin{aligned} \frac{\partial F_-}{\partial \tilde{m}} &= \kappa_{\rm a}\,(J - 4\pi B)\,, \\ \frac{\partial K_-}{\partial \tilde{m}} &= \frac{\kappa_{\rm a} F_+}{\beta_0^2}. \end{aligned} \tag{4.8}$$

Written in this form, it becomes easy to see why we define the *scattering parameter* as

$$\beta_0 \equiv \left(\frac{1-\omega_0}{1-\omega_0 g_0}\right)^{1/2}. \tag{4.9}$$

This is an important point—the single-scattering albedo and scattering asymmetry factor do not appear as independent quantities in equation (4.8). Rather, they are always combined in the form of β_0. For this reason, we will always describe the temperature-pressure profiles by the scattering parameter. In the shortwave, we will relate the scattering parameter to the Bond albedo, a quantity that may be inferred from astronomical observations.

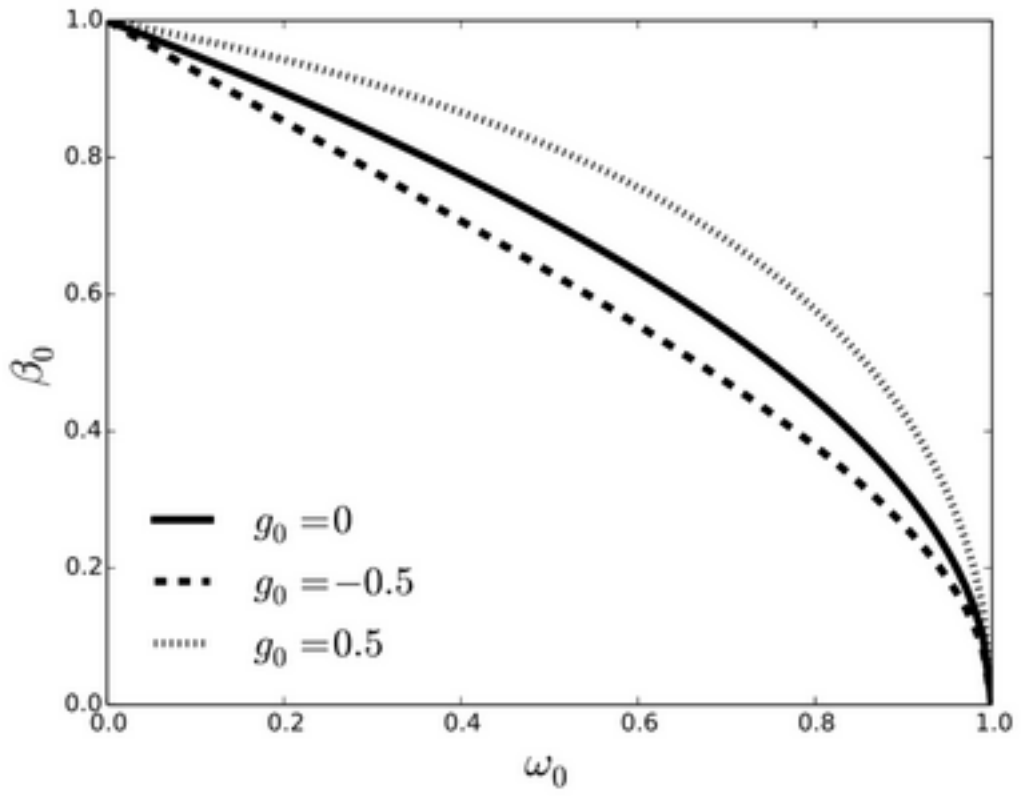

Figure 4.1: Scattering parameter as a function of the single-scattering albedo and scattering asymmetry factor. Pure absorption and scattering correspond to $\beta_0 = 1$ and 0, respectively. Isotropic, forward and backward scattering correspond to $g_0 = 0$, $g_0 > 0$ and $g_0 < 0$, respectively.

An atmosphere may be visualized as being a heat engine. The total amount of energy entering and leaving the atmosphere must be conserved. Integrated over wavelength, the energy content, per unit mass and time, of the atmosphere is

$$Q = \int_0^\infty \frac{\partial F_-}{\partial \tilde{m}}\, d\lambda = \frac{\partial \mathcal{F}_-}{\partial \tilde{m}} = \kappa_\mathrm{S} J_\mathrm{S} + \kappa_\mathrm{L} \left(J_\mathrm{L} - 4\sigma_\mathrm{SB} T^4 \right), \tag{4.10}$$

with $\mathcal{F}_-$ being the bolometric[2] net flux. The energy content, per unit area and time, of the atmosphere is derived from further integrating over the column mass,

$$\int_{\tilde{m}}^\infty \frac{\partial \mathcal{F}_-}{\partial \tilde{m}}\, d\tilde{m} = \tilde{Q}\left(\tilde{m}, \infty\right), \tag{4.11}$$

[2]Meaning integrated over all wavelengths, frequencies or wavenumbers.

where we have defined, for any arbitrary pair of column masses $\tilde{m}_1$ and $\tilde{m}_2$,

$$\tilde{Q}(\tilde{m}_1, \tilde{m}_2) \equiv \int_{\tilde{m}_1}^{\tilde{m}_2} Q \, d\tilde{m}. \tag{4.12}$$

Equations (4.10) and (4.11) allow for an alternative expression of radiative equilibrium, which occurs when $Q = 0$. This in turn implies that $\tilde{Q}(0, \infty) = 0$. Thus, the energy per unit area and time (i.e., the flux), integrated over all wavelengths and pressures, entering and exiting the atmosphere is conserved. Radiative equilibrium is a necessary and sufficient condition for global energy conservation. The converse is not true—global energy conservation does not guarantee radiative equilibrium, a point of contention among even professional researchers. Mathematically, the gradient of the bolometric net flux may conspire to be non-zero at multiple locations, only to cancel out when summed over the entire atmosphere, such that $\tilde{Q}(0, \infty) = 0$ but $Q \neq 0$.

By following through on equation (4.11), energy conservation may be expressed as

$$\begin{aligned} F_{\mathrm{L}} &= \mathcal{F}_\infty - F_{\mathrm{S}} - \tilde{Q}(\tilde{m}, \infty), \\ \epsilon_{\mathrm{L}} J_{\mathrm{L}_0} &= \mathcal{F}_\infty - F_{\mathrm{S}_0} - \tilde{Q}(0, \infty). \end{aligned} \tag{4.13}$$

For convenience, we have defined $F_{\mathrm{S}_0} \equiv F_{\mathrm{S}}(\tilde{m} = 0)$, $F_{\mathrm{L}_0} \equiv F_{\mathrm{L}}(\tilde{m} = 0)$ and $J_{\mathrm{L}_0} \equiv J_{\mathrm{L}}(\tilde{m} = 0)$. The bolometric net flux from the deep interior (as $\tilde{m} \to \infty$) is

$$\mathcal{F}_\infty = \sigma_{\mathrm{SB}} T_{\mathrm{int}}^4, \tag{4.14}$$

where σ_{SB} is the Stefan-Boltzmann constant. The quantity T_{int} is the *interior* or *internal temperature* and $\mathcal{F}_\infty$ should be regarded as a boundary condition of our model atmosphere. It describes the remnant heat of formation of an exoplanet.

4.4 TREATMENT OF SHORTWAVE RADIATION

4.4.1 Relationship between Bond albedo and scattering parameter

In the shortwave, stellar heating dominates and thermal emission from the exoplanet is negligible. We recall our two-stream solutions with non-isotropic scattering in equation (3.58). By considering incident starlight ($F_{\downarrow_1} \neq 0$, $F_{\uparrow_2} = 0$) upon an opaque atmosphere ($\mathcal{T} = 0$) and ignoring thermal emission in the shortwave ($B = 0$), we may use the two-stream solutions to derive the spherical albedo[3] [88, 94],

$$A_s \equiv \frac{F_{\uparrow_1}}{F_{\downarrow_1}} = \frac{1 - \beta_0}{1 + \beta_0}. \tag{4.15}$$

[3]Recall that opaqueness and reflectivity are independent attributes.

By integrating the spherical albedo over all wavelengths, we obtain the Bond albedo,

$$A_{\mathrm{B}} = \frac{1 - \beta_{\mathrm{S}_0}}{1 + \beta_{\mathrm{S}_0}}, \tag{4.16}$$

where β_{S_0} is the mean or characteristic value of β_0 in the shortwave. Since our two-stream solutions and temperature-pressure profiles have a common mathematical origin, this derivation is self-consistent.

4.4.2 Generalization of Beer's law

We now seek to obtain solutions for the total intensity and net flux in the shortwave and both recover and generalize Beer's law. When the governing equations in (4.4) are integrated over the shortwave, they become

$$\begin{aligned} \frac{\partial F_{\mathrm{S}}}{\partial \tilde{m}} &= \kappa_{\mathrm{S}} J_{\mathrm{S}}, \\ \frac{\partial K_{\mathrm{S}}}{\partial \tilde{m}} &= \frac{\kappa'_{\mathrm{S}} F_{\mathrm{S}}}{\beta_{\mathrm{S}_0}^2}, \end{aligned} \tag{4.17}$$

where the *absorption mean opacity* is [172]

$$\kappa_{\mathrm{S}} \equiv \frac{\int_{\mathrm{S}} \kappa_{\mathrm{a}} J \, d\lambda}{\int_{\mathrm{S}} J \, d\lambda}. \tag{4.18}$$

The *flux mean opacity* is

$$\kappa'_{\mathrm{S}} \equiv \frac{\int_{\mathrm{S}} \kappa_{\mathrm{a}} F_+ \, d\lambda}{\int_{\mathrm{S}} F_- \, d\lambda}. \tag{4.19}$$

We again have two equations and three unknowns (J_{S}, F_{S} and K_{S}). To proceed, we need a shortwave closure [79],

$$\epsilon_{\mathrm{S}} \equiv \frac{K_{\mathrm{S}}}{J_{\mathrm{S}}} = \mu^2, \tag{4.20}$$

where μ is the cosine of the polar angle or co-latitude. This form of the shortwave closure is chosen to correctly reproduce Beer's law in the limit of pure absorption and also generalize it to situations with scattering, as we will see shortly. In essence, we have guessed the form of the shortwave closure and validated our guess by reproducing Beer's law after the fact.

Drawing from the lessons of Chapter 3, we would like to combine the first-order differential equations in (4.17) into a single second-order differential equation, which behaves like an ordinary differential equation with $\tilde{m}$ being the independent variable. You will find that we cannot proceed unless we assume

$$\kappa_{\mathrm{S}} = \kappa'_{\mathrm{S}}. \tag{4.21}$$

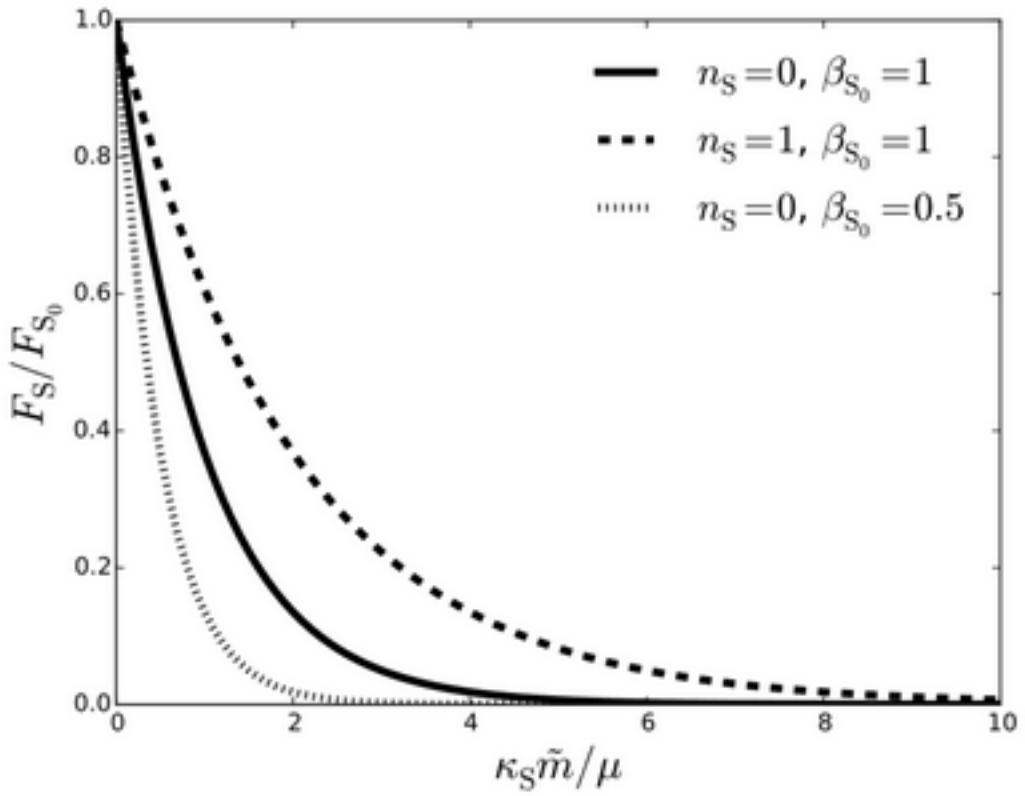

Figure 4.2: Generalization of Beer's law with non-isotropic scattering. The limit of constant shortwave opacity and pure absorption is given by $n_S = 0$ and $\beta_{S_0} = 1$. A steeper fall of the shortwave opacity with height allows for a deeper penetration of starlight ($n_S = 1$ and $\beta_{S_0} = 1$). Even when the shortwave opacity is constant, the presence of scattering causes a more rapid diminution of incident starlight ($n_S = 0$ and $\beta_{S_0} = 0.5$).

From this point onwards, we shall simply term κ_S the *shortwave opacity*. With this assumption, we obtain a pair of second-order ordinary differential equations,

$$\begin{aligned}\frac{\partial^2 J_S}{\partial \tilde{m}^2} - \frac{1}{\kappa_S}\frac{\partial \kappa_S}{\partial \tilde{m}}\frac{\partial J_S}{\partial \tilde{m}} - \left(\frac{\kappa_S}{\mu\beta_{S_0}}\right)^2 J_S = 0,\\ \frac{\partial^2 F_S}{\partial \tilde{m}^2} - \frac{1}{\kappa_S}\frac{\partial \kappa_S}{\partial \tilde{m}}\frac{\partial F_S}{\partial \tilde{m}} - \left(\frac{\kappa_S}{\mu\beta_{S_0}}\right)^2 F_S = 0.\end{aligned} \tag{4.22}$$

When κ_S is constant, the pesky first derivatives in equation (4.22) vanish and the solutions are straightforward to obtain. What is surprising and less obvious is that a power-law form of the shortwave opacity,

$$\kappa_S = \kappa_{S_0}\left(\frac{\tilde{m}}{\tilde{m}_0}\right)^{n_S}, \tag{4.23}$$

where $\tilde{m}_0$ is a reference value of the column mass usually set to correspond to the bottom of atmosphere, admits the following analytical solutions [94],

$$J_S = J_{S_0} e^{\beta_S/\mu},\ F_S = F_{S_0} e^{\beta_S/\mu}, \tag{4.24}$$

with $J_{S_0} \equiv J_S(\tilde{m} = 0)$, $F_{S_0} \equiv F_S(\tilde{m} = 0)$ and

$$\beta_S \equiv \frac{\kappa_S \tilde{m}}{(n_S + 1)\,\beta_{S_0}}. \tag{4.25}$$

Since the column mass increases with pressure, a larger value of the index n_S means that starlight is able to penetrate deeper into the atmosphere. Mathematically, there are two solution branches, but we have picked the one that allows J_S and F_S to vanish as $\tilde{m} \to \infty$, because we expect starlight to be completely attenuated if it penetrates deeply enough into the atmosphere.

When the shortwave opacity is constant ($n_S = 0$) and scattering is absent ($\beta_{S_0} = 1$), we see that equation (4.24) correctly reproduces the classical version of Beer's law. Otherwise, equation (4.24) provides a generalization of Beer's law that includes the effects of non-isotropic scattering [94]. Figure 4.2 shows examples of the diminution of shortwave flux with different combinations of values for n_S and β_{S_0}. Generally, the presence of scattering ($\beta_{S_0} < 1$) causes a more rapid diminution of incident starlight within an atmosphere.

4.4.3 The photon deposition depth

With the generalization of Beer's law in hand, we are now in a position to locate the atmospheric layer at which most of the starlight is being absorbed. We shall term this layer the *photon deposition depth* [88, 94]. We seek a relationship between the pressure (P_D) corresponding to the photon deposition depth/layer and the Bond albedo.

The shortwave flux at $\tilde{m} = 0$ is interpreted as the incident stellar flux,

$$F_{S_0} = \mu F_\star, \tag{4.26}$$

where the *stellar constant*[4] is

$$F_\star \equiv \begin{cases} \sigma_{SB} T_{irr}^4, & 0 \le \phi \le \pi, \\ 0, & \pi \le \phi \le 2\pi, \end{cases} \tag{4.27}$$

and the *irradiation temperature* is

$$T_{irr} = T_\star \left(\frac{R_\star}{a}\right)^{1/2} (1 - A_B)^{1/4} = \sqrt{2} T_{eq}. \tag{4.28}$$

It is the temperature at the substellar point of an exoplanet, which is the point where the distance between itself and the star is the shortest.

It is important to note that $F_{S_0} < 0$ arises naturally from the fact that it is a *net flux with a vanishing outgoing component.* By using the expression for F_S from equation (4.24), we find that the mean value of the shortwave net flux is

$$\bar{F}_S \equiv \frac{1}{2\pi} \int_0^{2\pi} \int_{-1}^{0} F_S \, d\mu \, d\phi = -\frac{\sigma_{SB} T_{irr}^4 \mathcal{E}_3}{2}, \tag{4.29}$$

[4]Generalized from the *solar constant.*

where $\mathcal{E}_3 = \mathcal{E}_3(\beta_S)$ and the exponential integral of the jth order is defined as [2, 7]

$$\mathcal{E}_j(\beta_S) \equiv \int_1^\infty x^{-j} e^{-x\beta_S}\, dx. \tag{4.30}$$

By denoting $\bar{F}_{S_0} \equiv \bar{F}_S(\tilde{m} = 0)$, it follows that

$$\frac{\bar{F}_S}{\bar{F}_{S_0}} = 2\mathcal{E}_3. \tag{4.31}$$

We define the photon deposition depth as the pressure level where $\bar{F}_S/\bar{F}_{S_0}$ suffers one e-folding, i.e., is equal to about 0.368, which occurs when $\beta_S \approx 0.63$. It follows that

$$\begin{aligned} P_D &= \left[\frac{0.63\,(n_S+1)\,gP_0^{n_S}}{\kappa_{S_0}}\right]^{1/(n_S+1)} \left(\frac{1-\omega_{S_0}}{1-\omega_{S_0}g_{S_0}}\right)^{1/2(n_S+1)} \\ &= \left[\frac{0.63\,(n_S+1)\,gP_0^{n_S}}{\kappa_{S_0}}\right]^{1/(n_S+1)} \left(\frac{1-A_B}{1+A_B}\right)^{1/(n_S+1)}, \end{aligned} \tag{4.32}$$

where ω_{S_0} and g_{S_0} are the mean or characteristic values of the single-scattering albedo and scattering asymmetry factor in the shortwave, respectively. The pressure corresponding to the bottom[5] of the atmosphere is $P_0 = \tilde{m}_0 g$ and g is the surface gravity of the exoplanet.

The photon deposition depth has the expected physical property that, as the scattering becomes more backward-peaked ($g_{S_0} < 0$), it resides higher up in the atmosphere. As $n_S \to \infty$, $P_D \to P_0$. When $n_S = 0$, the expression for P_D is particularly useful because it is independent of P_0. For pure forward scattering ($g_{S_0} = 1$), photon deposition behaves as if one is in the purely absorbing limit. Backward scattering ($g_{S_0} = -1$) tends to raise the photon deposition depth to higher altitudes (lower pressures).

4.5 TREATMENT OF LONGWAVE RADIATION

The governing equations in the longwave are

$$\begin{aligned} \frac{\partial F_L}{\partial \tilde{m}} &= \kappa_L J_L - 4\kappa_L'' \sigma_{SB} T^4, \\ \frac{\partial K_L}{\partial \tilde{m}} &= \frac{\kappa_L' F_L}{\beta_{L_0}^2}, \end{aligned} \tag{4.33}$$

where T is the temperature. Unlike in the shortwave, the longwave equations include blackbody emission from the exoplanetary atmosphere. The absorption, flux and Planck mean opacities are, respectively,

$$\kappa_L \equiv \frac{\int_L \kappa_a J\, d\lambda}{\int_L J\, d\lambda},\quad \kappa_L' \equiv \frac{\int_L \kappa_a F_+\, d\lambda}{\int_L F_-\, d\lambda},\quad \kappa_L'' \equiv \frac{\pi \int_L \kappa_a B\, d\lambda}{\sigma_{SB} T^4}. \tag{4.34}$$

[5]This really means the bottom of the model domain, since it is unclear if gas-giant exoplanets, for example, have a "bottom."

As before, we need to combine the pair of governing equations. In order to proceed, we have to assume that $\kappa_{\rm L} = \kappa'_{\rm L} = \kappa''_{\rm L}$. We shall term $\kappa_{\rm L}$ the *longwave opacity*.

Now, we have two equations and *four* unknowns ($J_{\rm L}$, $F_{\rm L}$, $K_{\rm L}$ and T). Since we are ultimately interested in the temperature, we need two more Eddington coefficients,

$$\epsilon_{\rm L} \equiv \frac{F_{\rm L}}{J_{\rm L}} = \frac{3}{8}, \; \epsilon_{\rm L_3} \equiv \frac{K_{\rm L}}{J_{\rm L}} = \frac{1}{3}. \tag{4.35}$$

Problem 4.9.1 will teach you how to derive the values of these *longwave Eddington coefficients*, based on what we learned in Chapter 3. You will often encounter studies that assume the first longwave Eddington coefficient to be $\epsilon_{\rm L} = 1/2$, which is inconsistent with the values we assume for the other Eddington coefficients.

4.6 ASSEMBLING THE PIECES: DERIVING THE GENERAL SOLUTION

We are finally ready to assemble the various pieces we painstakingly constructed and derive the temperature-pressure profile of an irradiated atmosphere with a finite remnant heat of formation. By combining the second equation in (4.33), the first equation in (4.13) and using the third longwave Eddington coefficient, we obtain

$$J_{\rm L} = J_{\rm L_0} + \frac{1}{\epsilon_{\rm L_3}\beta^2_{\rm L_0}} \int_0^{\tilde{m}} \kappa_{\rm L} \left[\mathcal{F}_\infty - F_{\rm S} - \tilde{Q}\left(\tilde{m}, \infty\right) \right] \, d\tilde{m}. \tag{4.36}$$

Eliminating the quantities $J_{\rm L}$ and $J_{\rm L_0}$ using equation (4.10) and the second equation in (4.13), respectively, yields

$$\begin{aligned} \sigma_{\rm SB} T^4 = & \frac{\mathcal{F}_\infty}{4} \left(\frac{1}{\epsilon_{\rm L}} + \frac{1}{\epsilon_{\rm L_3}\beta^2_{\rm L_0}} \int_0^{\tilde{m}} \kappa_{\rm L} \, d\tilde{m} \right) + \mathcal{Q} \\ & + \frac{1}{4} \left(- \frac{F_{\rm S_0}}{\epsilon_{\rm L}} + \frac{\kappa_{\rm S} J_{\rm S}}{\kappa_{\rm L}} - \frac{1}{\epsilon_{\rm L_3}\beta^2_{\rm L_0}} \int_0^{\tilde{m}} \kappa_{\rm L} F_{\rm S} \, d\tilde{m} \right). \end{aligned} \tag{4.37}$$

At this point, it is worth pausing and understanding the physical significance of each term in equation (4.37). The first term, involving $\mathcal{F}_\infty$, is the generalization of Milne's solution to a situation with non-isotropic scattering [94]. It is equivalent to the diffusion solution we derived in Chapter 3. The second term collects all of the terms associated with Q,

$$\mathcal{Q} \equiv -\frac{1}{4} \left[\frac{Q}{\kappa_{\rm L}} + \frac{\tilde{Q}\left(0, \infty\right)}{\epsilon_{\rm L}} + \frac{1}{\epsilon_{\rm L_3}\beta^2_{\rm L_0}} \int_0^{\tilde{m}} \kappa_{\rm L} \tilde{Q}\left(\tilde{m}, \infty\right) \, d\tilde{m} \right]. \tag{4.38}$$

The rest of the terms are associated with the stellar heating of the atmosphere.

Towards the end of Chapter 3, we saw that Milne's solution, derived in the diffusion limit, uses the Rosseland mean opacity. In the current derivation, we have assumed that the absorption, flux and Planck mean opacities are equal. That we end up with Milne's solution via both approaches can only imply that these three arithmetic means are equal to the harmonic mean, which is a strong assumption because they lend very different weights to the smallest and largest opacities across a wavelength range. In our bid to derive an analytical model, we expectedly paid the price of forgoing physical realism.

We obtain the global-mean temperature-pressure profile by integrating over all possible incident angles of starlight ($0 \leq \phi \leq 2\pi$ and $-1 \leq \mu \leq 0$) and dividing by 2π,

$$\begin{aligned}\bar{T}^4 =& \frac{T_{\rm int}^4}{4}\left(\frac{1}{\epsilon_{\rm L}} + \frac{1}{\epsilon_{\rm L_3}\beta_{\rm L_0}^2}\int_0^{\tilde{m}} \kappa_{\rm L}\, d\tilde{m}\right) \\ &+ \frac{T_{\rm irr}^4}{8}\left(\frac{1}{2\epsilon_{\rm L}} + \frac{\kappa_{\rm S}\mathcal{E}_2}{\kappa_{\rm L}\beta_{\rm S_0}} + \frac{1}{\epsilon_{\rm L_3}\beta_{\rm L_0}^2}\int_0^{\tilde{m}} \kappa_{\rm L}\mathcal{E}_3\, d\tilde{m}\right) \\ &+ \frac{1}{2\pi}\int_0^{2\pi}\int_{-1}^{0} \mathcal{Q}\, d\mu\, d\phi,\end{aligned} \tag{4.39}$$

where we again have $\mathcal{E}_j(\beta_{\rm S})$ being the exponential integral of the j-th order. The last term in equation (4.39) vanishes when radiative equilibrium *and* global energy conservation are attained.

To evaluate the integral involving the longwave opacity, we assume its functional form to be

$$\kappa_{\rm L} = \kappa_0 + \kappa_{\rm CIA}\left(\frac{\tilde{m}}{\tilde{m}_0}\right), \tag{4.40}$$

where κ_0 and $\kappa_{\rm CIA}$ are constants. The physical significance of this functional form will be explained shortly. If we also assume a constant shortwave opacity ($n_{\rm S} = 0$), then we end up with a fully explicit expression for the temperature-pressure profile,

$$\begin{aligned}\bar{T}^4 =& \frac{T_{\rm int}^4}{4}\left[\frac{1}{\epsilon_{\rm L}} + \frac{\tilde{m}}{\epsilon_{\rm L_3}\beta_{\rm L_0}^2}\left(\kappa_0 + \frac{\kappa_{\rm CIA}\tilde{m}}{2\tilde{m}_0}\right)\right] \\ &+ \frac{T_{\rm irr}^4}{8}\left[\frac{1}{2\epsilon_{\rm L}} + \mathcal{E}_2\left(\frac{\kappa_{\rm S}}{\kappa_{\rm L}\beta_{\rm S_0}} - \frac{\kappa_{\rm CIA}\tilde{m}\beta_{\rm S_0}}{\epsilon_{\rm L_3}\kappa_{\rm S}\tilde{m}_0\beta_{\rm L_0}^2}\right)\right. \\ &\left. + \frac{\kappa_0\beta_{\rm S_0}}{\epsilon_{\rm L_3}\kappa_{\rm S}\beta_{\rm L_0}^2}\left(\frac{1}{3} - \mathcal{E}_4\right) + \frac{\kappa_{\rm CIA}\beta_{\rm S_0}^2}{\epsilon_{\rm L_3}\kappa_{\rm S}^2\tilde{m}_0\beta_{\rm L_0}^2}\left(\frac{1}{2} - \mathcal{E}_3\right)\right].\end{aligned} \tag{4.41}$$

With this formula, we are now ready to explore the basic trends associated with temperature-pressure profiles.

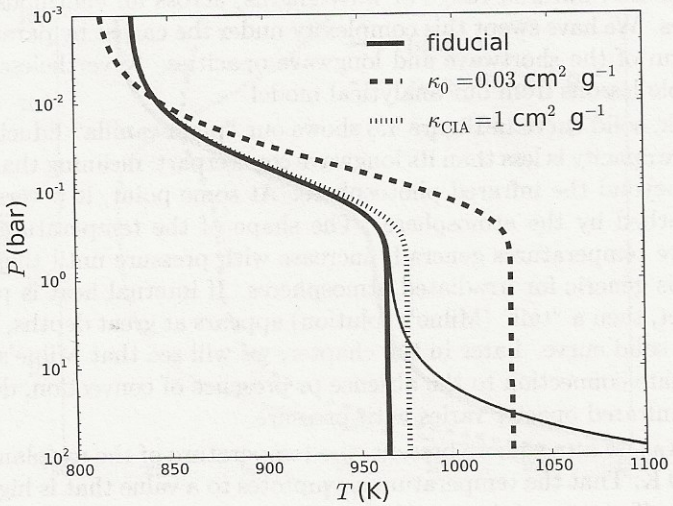

Figure 4.3: Elucidating the effects of greenhouse warming using temperature-pressure profiles in the purely absorbing limit. The fiducial model (thick, solid curve) has the following parameter values: $T_{\rm int} = 0$, $T_{\rm irr} = 1200$ K, $g = 10^3$ cm s^{-2}, $n_{\rm S} = 0$, $\kappa_{\rm S_0} = 0.01$ cm^2 g^{-1}, $\kappa_0 = 0.02$ cm^2 g^{-1}, $\kappa_{\rm CIA} = 0$, $\beta_{\rm S_0} = 1$ and $\beta_{\rm L_0} = 1$. The other models modify one of the parameter values as stated in the legend. The thin, solid curve is the fiducial model recomputed with $T_{\rm int} = 150$ K and shows Milne's solution.

4.7 EXPLORATION OF DIFFERENT ATMOSPHERIC EFFECTS

Our analytical model of the temperature-pressure profile of an atmosphere allows us to perform controlled experiments to understand the effects of varying the various parameters, much like how one does an experiment in the laboratory. To this end, we create a fiducial model with the following properties: constant opacities, no scattering in either the shortwave or longwave and the absence of collision-induced absorption. Its parameter values are listed in the caption of Figure 4.3. Based on this fiducial model, we selectively modify one parameter at a time in order to isolate its effect. Such an approach is the basis of good theory, at least in astrophysics.

4.7.1 Greenhouse warming

The gaseous component of a real atmosphere is composed of a soup of atoms and molecules, each with an ability to absorb radiation via the laws of quantum mechanics. Typically, molecules absorb photons via ro-vibrational transitions

in the visible and infrared range of wavelengths, across an enormous array of spectral lines. We have swept this complexity under the carpet by parametrizing it in the form of the shortwave and longwave opacities. Nevertheless, we may learn valuable lessons from our analytical model.

The thick, solid curve in Figure 4.3 shows our "plain vanilla" fiducial model. Its shortwave opacity is less than its longwave counterpart, meaning that starlight penetrates beyond the infrared photosphere. At some point, it peters out and is fully absorbed by the atmosphere. The shape of the temperature-pressure profile, where temperatures generally increase with pressure until they become isothermal, is generic for irradiated atmospheres. If internal heat is present in the exoplanet, then a "tail" (Milne's solution) appears at great depths, as shown by the thin, solid curve. Later in the chapter, we will see that Milne's solution has an intimate connection to the absence or presence of convection, depending on how the infrared opacity varies with pressure.

If there was no atmosphere present, the temperature of the exoplanet would be about 850 K. That the temperature asymptotes to a value that is higher than 850 K is a manifestation of the *greenhouse effect*—starlight enters an atmosphere with relative ease, but thermal emission has greater difficulty escaping due to an enhanced infrared opacity, exactly like how a greenhouse functions.

The thick, dashed curve in Figure 4.3 shows that increasing the longwave or infrared opacity has the effect of strengthening the greenhouse warming. It is apparent that this warms the lower atmosphere and cools the upper atmosphere.

4.7.2 Collision-induced absorption

Symmetrically diatomic molecules such as hydrogen or nitrogen do not possess permanent dipole moments and thus are unable, to lowest order, to absorb radiation. However, at high pressures ($\gtrsim$ 1 bar) two molecules of hydrogen or nitrogen may come together and form a transient "super-molecule" with a weak quadrupole moment, which then absorbs radiation. This effect is known as *collision-induced absorption* (CIA). It is typically weak, but if it is the only game in town, then it becomes noticeable. In fact, CIA was first observed in the hydrogen-dominated atmospheres of Uranus and Neptune in the 1950s [102].

The functional form of the longwave opacity, as stated in equation (4.40), becomes clear. It consists of a constant component for the greenhouse gases (e.g., water, methane, carbon monoxide) and a linear component to mimic CIA associated with the inert buffer gas. Since CIA is a two-body process, we expect the optical depth to be proportional to the square of the number density of the atmospheric gas. This is reflected in our prescription that the optical depth associated with CIA is $\tau_{\rm CIA} \propto P^2$.

The thick, dotted curve in Figure 4.3 examines the effects of "switching on" CIA, which warms the atmosphere everywhere compared to the fiducial model and especially at high pressures. Unlike the pressure broadening of spectral lines, CIA is a continuum effect that occurs across a broad range of wavelengths. It

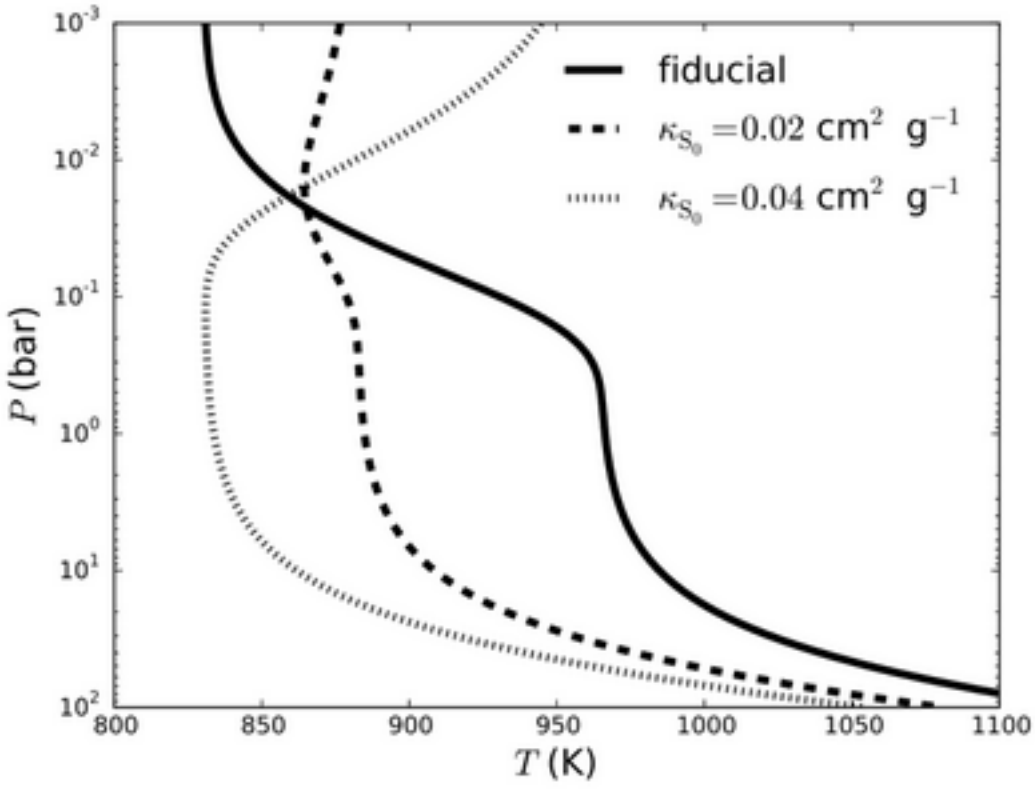

Figure 4.4: Elucidating the effects of anti-greenhouse cooling using temperature-pressure profiles in the purely absorbing limit. In this set of models, we have set $T_{\rm int} = 150$ K. The thick, dashed curve has the shortwave and longwave opacities being equal. The thick, dotted curve has $\kappa_{S_0}/\kappa_0 = 2$.

is generally difficult to calculate the opacity associated with CIA, as it depends on the nature[6] of the collidants and the ambient pressure [1].

4.7.3 Anti-greenhouse cooling and atmospheric inversions

What happens when we increase the shortwave opacity to the point where it becomes larger than its longwave counterpart? Physically, this is akin to inserting extra absorbers of shortwave radiation in the atmosphere. On Earth, this role is played by ozone in the ultraviolet range of wavelengths. On exoplanets, a favored guess of the astronomers is titanium monoxide (TiO), due to its prevalence in the observed spectra of brown dwarfs [116], although it remains to be seen if the analogy between brown dwarfs and gas-giant exoplanets carries this far.

The thick, dashed and dotted curves in Figure 4.4 illustrate the effect of increasing the shortwave opacity to the point where it dominates the longwave opacity, which leads to the *anti-greenhouse effect*—the upper atmosphere warms and the lower atmosphere cools. The onset of the isothermal component shifts to lower pressures, since starlight is now deposited at higher altitudes. The

[6]More specifically, it depends on the stoichiometry of the collidants. For example, CIA may occur between a pair of hydrogen molecules or between a hydrogen molecule and a helium atom.

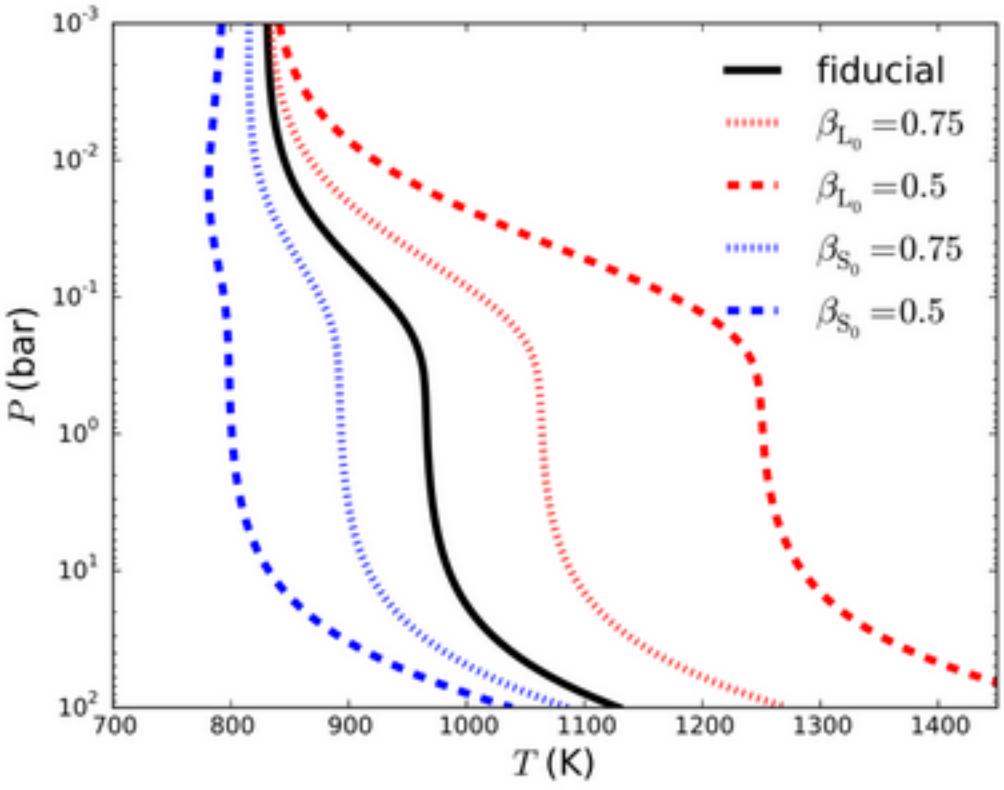

Figure 4.5: Elucidating the effects of shortwave/optical and longwave/infrared scattering on the temperature-pressure profiles. As the scattering parameter decreases, the strength of scattering increases. Shortwave scattering enhances the anti-greenhouse effect, while longwave scattering generally warms the entire atmosphere. In this set of models, we have also set $T_{\rm int} = 150$ K.

thick, dotted curve develops a *temperature inversion*, where temperature now increases with altitude.

There is a long and rich debate in the astrophysical literature on the possible existence of temperature inversions in exoplanetary atmospheres [27, 28, 63, 64, 124, 152, 153, 155, 171, 229], although the shortwave absorber has yet to be clearly identified. If temperature inversions are present, they may negate the effects of disequilibrium chemistry by warming the upper atmosphere [175]—chemical time scales tend to be shorter at higher temperatures. This has consequences for interpreting chemical abundances.

4.7.4 Albedo variations

An important and measurable quantity is the Bond albedo of the atmosphere, which is the fraction of incident starlight reflected away from it across all wavelengths. The Bond albedo essentially controls the energy budget of an atmosphere. It is generally mediated by the presence of aerosols, condensates or dust grains, whose chemistry and compositions are not always easy to decipher. Nevertheless, it is of interest to understand the effects of a varying albedo on the thermal structure of an atmosphere.

One each of the thick, dotted and dashed curves in Figure 4.5 are for model

atmospheres with shortwave scattering parameters of 0.75 and 0.5, respectively. In terms of the Bond albedo, these correspond to $A_{\rm B} = 1/7 \approx 14\%$ and $A_{\rm B} = 1/3 \approx 33\%$. A finite albedo exerts an effect similar to that of anti-greenhouse cooling, but with a key difference—not only do the upper and lower parts of the atmosphere warm and cool, respectively, the entire temperature-profile shifts to lower temperatures because of the $(1 - A_{\rm B})^{1/4}$ factor present in the irradiation temperature. In other words, the total energy content of the atmosphere is reduced by a factor of $(1 - A_{\rm B})$.

4.7.5 Scattering greenhouse effect

When scattering in the longwave or infrared is present, the opposite effect occurs—the atmosphere is warmer everywhere, as shown by the other set of thick, dotted and dashed curves in Figure 4.5. Thermal emission from the exoplanetary atmosphere attempts to escape, but some of it is scattered back into the exoplanet. This is known as the *scattering greenhouse effect*. If the thermal emission occurs predominantly in the infrared, then large particles (micron-sized or larger) are required for it to be noticeable.

Overall, the reason why aerosols or clouds, when they are present in an atmosphere, complicate any analysis or interpretation is that they are capable of exerting some combination of all of these effects: greenhouse warming and anti-greenhouse cooling in the form of both absorption and scattering. As we have seen, each of these effects has a significant influence on the thermal structure of an atmosphere. Sometimes, they reinforce each other; at other times, they cancel each other out. It is often difficult to accurately account for all of these effects in a real atmosphere, even in the presence of observational constraints.

4.8 MILNE'S SOLUTION AND THE CONVECTIVE ADIABAT

If an exoplanet possesses an internal source of heat, then it is possible that convection is active deep within its atmosphere. In our temperature-pressure profiles, this deep component is Milne's solution. It is worth investigating whether it is unstable to convection—and if so, to clarify the conditions under which convection is triggered.

If you work through Chapter 12 and Problem 12.9.1, then you will convince yourself that the atmosphere is stable against convection if *Schwarzschild's criterion* is fulfilled,

$$\frac{\partial \left(\ln \bar{T} \right)}{\partial \left(\ln P \right)} \leq \kappa_{\rm ad} = \frac{2}{2 + n_{\rm dof}}, \tag{4.42}$$

where $\kappa_{\rm ad}$ is the adiabatic gradient. The criterion depends on the number of degrees of freedom ($n_{\rm dof}$) of the dominant atmospheric gas, which is generally a function of both chemical composition and temperature. If we include translation, rotation and vibration, then a diatomic molecule would have $n_{\rm dof} = 6$ and $\kappa_{\rm ad} = 1/4$. If we exclude vibration, then $\kappa_{\rm ad} = 2/7$. In what follows, we

will assume that the buffer gas of the atmosphere is diatomic, which is not an unreasonable assumption—molecular nitrogen is the dominant gas, by mass, for the atmospheres of Earth and Titan, while molecular hydrogen seems to be the buffer gas of choice for Jupiter, Saturn and many detected exoplanets.

By differentiating Milne's solution with respect to pressure, we obtain

$$\frac{\partial\left(\ln\bar{T}\right)}{\partial\left(\ln P\right)}=\frac{P}{4\epsilon_{\mathrm{L}_3}\beta_{\mathrm{L}_0}^2 g}\left(\kappa_0+\frac{\kappa_{\mathrm{CIA}}P}{P_0}\right)\left(\frac{1}{\epsilon_{\mathrm{L}}}+\frac{\kappa_0 P}{\epsilon_{\mathrm{L}_3}\beta_{\mathrm{L}_0}^2 g}+\frac{\kappa_{\mathrm{CIA}}P^2}{2\epsilon_{\mathrm{L}_3}\beta_{\mathrm{L}_0}^2 P_0 g}\right)^{-1}. \tag{4.43}$$

At high pressures, this dimensionless temperature gradient becomes

$$\lim_{P\to\infty}\frac{\partial\left(\ln\bar{T}\right)}{\partial\left(\ln P\right)}=\begin{cases}\frac{1}{4}, & \kappa_{\mathrm{CIA}}=0,\\ \frac{1}{2}, & \kappa_0=0.\end{cases} \tag{4.44}$$

These asymptotic values lead us to a remarkable conclusion, independent of the strength of absorption or scattering in the infrared and the surface gravity of the exoplanet—if collision-induced absorption is operating deep in the atmosphere, then Milne's solution is unconditionally unstable to convection. In this situation, it describes the fully-convective interior of an exoplanet (e.g., a gas giant). If collision-induced absorption is inactive, then it is unconditionally stable to convection.

These considerations highlight an equally remarkable aspect of atmospheres: opacities, determined by the laws of quantum physics, are conspiring with thermodynamics and fluid dynamics, via Schwarzschild's criterion, to produce convective mixing, a distinctively macroscopic phenomenon. It is a stark reminder that to understand exoplanetary atmospheres, a holistic approach is needed.

4.9 PROBLEM SETS

4.9.1 The longwave Eddington coefficients

To use the formula for the temperature-pressure profile, one needs to fix the values of the first and third longwave Eddington coefficients. The latter is easy and follows directly from the third Eddington coefficient: $\epsilon_{\mathrm{L}_3}=\epsilon_3=1/3$. For the former, show, using the two expressions for ϵ_2, that

$$F_-=\frac{F_+^2}{2K_-}. \tag{4.45}$$

Hence, show that

$$\epsilon_{\mathrm{L}}\equiv\frac{F_-}{J}=\frac{\epsilon^2}{2\epsilon_3}=\frac{3}{8}. \tag{4.46}$$

Here, we have not used the subscript "L" in order to distinguish clearly between the net and total fluxes.

4.9.2 Detached convective regions

Higher up in the atmosphere, stellar irradiation generally acts to reduce the lapse rate and stabilize it against convection. However, if the shortwave opacity is sufficiently smaller than its longwave counterpart, such that the greenhouse effect is strong, it is possible to have *detached convective regions* straddled by zones of stability.

Consider a temperature-pressure profile, in the purely absorbing limit, with a constant shortwave opacity, no internal heat and a longwave opacity only due to collision-induced absorption,

$$\bar{T}^4 = \frac{T_{\rm irr}^4}{8}\left[\frac{1}{2\epsilon_{\rm L}} + \mathcal{E}_2\left(\frac{\kappa_{\rm S}}{\kappa_{\rm L}} - \frac{\kappa_{\rm CIA}\tilde{m}}{\epsilon_{\rm L_3}\kappa_{\rm S}\tilde{m}_0}\right) + \frac{\kappa_{\rm CIA}}{\epsilon_{\rm L_3}\kappa_{\rm S}^2\tilde{m}_0}\left(\frac{1}{2} - \mathcal{E}_3\right)\right]. \qquad (4.47)$$

(a) Derive the expression for $\frac{\partial(\ln \bar{T})}{\partial(\ln P)}$.

(b) What is the value of $\frac{\partial(\ln \bar{T})}{\partial(\ln P)}$ as $P \to \infty$?

(c) Compute the graphical solution of $\frac{\partial(\ln \bar{T})}{\partial(\ln P)}$ for $P_0 = 100$ bar, $g = 10^3$ cm s^{-2}, $\kappa_{\rm S} = 0.001$ cm^2 g^{-1} and $\kappa_{\rm CIA} = 0.01, 0.1$ and 1 cm^2 g^{-1}. Are there regions of convective instability within each model atmosphere?

4.9.3 Non-constant shortwave opacity

Write a `Python` program to compute temperature-pressure profiles for $n_{\rm S} = 0, 0.5$ and 1. What is the main qualitative difference between these profiles?